A Charge-Based Compact Model of Double Gate MOSFET

A. S. Roy[1], C. C. Enz[1,2] and J. M. Sallese[1]

1 Ecole Polytechnique Fdrale de Lausanne (EPFL), anandasankar.roy@epfl.ch, Jean-Michel.Sallese@epfl.ch
2 Swiss Center for Electronics and Microtechnology (CSEM), christian.enz@csem.ch

ABSTRACT

Although both exact and design oriented approximate closed-form analytical solution of the drain current for the symmetric double gate (DG) MOST exist, a closed-form expression for asymmetric DG MOST is still lacking. In this context, this work presents a semi-empirical analytic closed-form charge-based expression for the drain current of asymmetric DG MOST that is valid from weak to strong inversion and retains the asymptotic behavior. In addition, important small-signal quantities such as the transconductance-to-current ratio are readily obtained and reveal that these are nearly insensitive to the degree of asymmetry.

1 Introduction

Double gate (DG) MOST has several intrinsic advantages (i.e. almost ideal subthreshold slope, higher on to off current ratio and reduced short channel effect) over bulk MOST [1]. A good compact model for DG MOSFET is a prerequisite to actually exploit those advantages in integrated circuits. To date, a simple physical compact model is still lacking even for the 'classical' asymmetric DG MOST because of it's relatively complex electrostatics. Ref [2] has presented an exact solution for the symmetric DG MOST but it does not yield a closed form solution for the drain current for the asymmetric case, which is essential in order to have a compact model. To the best of our knowledge this is the only approach which can provide drain current for an asymmetric MOST with a good accuracy. The approach of [2]requires numerical integration and solving of two very complicated coupled nonlinear equations at each discretization point across the channel. The main purpose of this work is to eliminate the need for numerical integration. At the end one needs to solve numerically only for the source and the drain end charge and not for all the discretization points along the channel.

In this work we first prove that a symmetrical relation between the common mode gate voltage and the channel potential exists for a DG MOST. This feature is unique to DG MOST in contrast to the bulk MOST and will be used to obtain a closed form expression of the drain current. We will show that thanks to this symmetry, it is possible to describe the non-equilibrium transport of the DG MOST in terms of its equilibrium relationships. Then we will handle the equilibrium electrostatics in a piece-wise way and by suitable interpolation we will propose a semi-empirical analytic closed form charge-based expression for the drain current for both symmetrical and asymmetrical operation of the DG MOST.

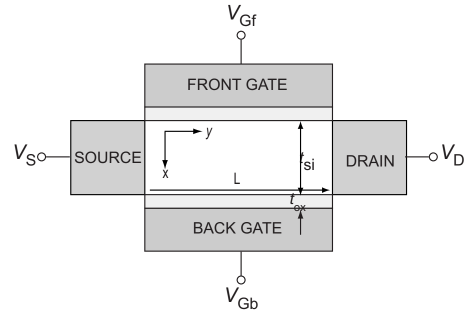

Figure 1: Schematic diagram of a DG MOSFET.

2 The symmetry between common mode gate voltage and channel potential

In equilibrium, the potential of the channel gets determined by the Poisson equation which is

$$\frac{d^2\Psi}{dx^2} = -\rho = f(\Psi, x), \quad (1)$$

where x is the distance across the silicon thickness (see Fig.1). In presence of a channel potential V, the Poisson equation changes to

$$\frac{d^2\Psi}{dx^2} = f(\Psi - V, x). \quad (2)$$

Assuming that the channel potential does not change along the vertical direction, i.e. x, and introducing a quantity $\widetilde{\Psi}$ defined as

$$\widetilde{\Psi} = \Psi - V, \quad (3)$$

we find that $\widetilde{\Psi}$ satisfies the equilibrium Poisson equation. Next, we note that the gate voltage dependence of Ψ comes from the continuity of displacement vector at the silicon-oxide interface (since Poisson equation is a 2nd order ODE, the two integration constants are evaluated from the boundary conditions at the two silicon-oxide interfaces).V_G always comes with a functional form of $V_G - \Psi$ because the electric field at the interface is simply $\varepsilon_{ox}(V_G - \Psi)/t_{ox}$. Since

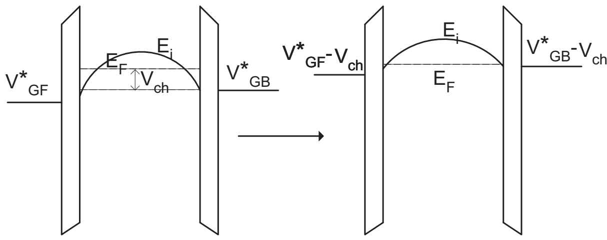

Figure 2: Effect of a channel potential in energy band diagram for a asymmetric MOST. This effect can re reduced to an equilibrium situation using gate voltages $V^*_{Gf(b)} - V$.

$V_G - \Psi = V_G - V - \widetilde{\Psi}$, $\widetilde{\Psi}$ actually 'sees' $V_G - V$ instead of V_G in the boundary condition. This implies that if Ψ has an equilibrium solution of the form of $\Psi_{eq}(V^*_{Gf}, V^*_{Gb})$, (where $V^*_{Gf(b)} = V_{Gf(b)} - \Delta_{f(b)}$ is the effective front(back) voltage including the work function difference $\Delta_{f(b)}$), then $\widetilde{\Psi}$ is given by

$$\widetilde{\Psi}(V^*_{Gf}, V^*_{Gb}, V) = \Psi_{eq}(V^*_{Gf} - V, V^*_{Gb} - V). \quad (4)$$

From the definition of $\widetilde{\Psi}$, the potential in non-equilibrium can be obtained as

$$\Psi(V^*_{Gf}, V^*_{Gb}, V) = V + \Psi_{eq}(V^*_{Gf} - V, V^*_{Gb} - V). \quad (5)$$

After finding the potential in the channel we can easily find out the front gate charge Q_f, the back gate charge Q_b, and the total inversion charge Q_i as

$$Q_f = C_{oxf}(V^*_{Gf} - \Psi_f) \quad (6a)$$

$$Q_b = C_{oxb}(V^*_{Gb} - \Psi_b) \quad (6b)$$

$$Q_i = Q_f + Q_b, \quad (6c)$$

where $\Psi_{f(b)}$ is the potential at the front(back) surface and $C_{oxf(b)}$ is the front(back) gate capacitance per unit area. From (5) and (6) it follows that for all Q_f, Q_b and Q_i we have

$$Q(V^*_{Gf}, V^*_{Gb}, V) = Q_{eq}(V^*_{Gf} - V, V^*_{Gb} - V), \quad (7)$$

where Q_{eq} is the corresponding equilibrium charge. In Fig. 2 we show the situation in energy band diagram which demonstrates that the presence of a channel potential can be simply considered as a shift in both of the gate voltages. Now if we rewrite the equilibrium charge in terms of the common mode and the difference mode gate voltage we have

$$Q(V^*_{Gf}, V^*_{Gb}, V) = Q_{eq}(V_{CM} - V, V_{DM}), \quad (8)$$

where $V_{CM} = (V^*_{Gf} + V^*_{Gb})/2$ and $V_{DM} = (V^*_{Gf} - V^*_{Gb})/2$. Now the current under drift diffusion assumption is given by

$$I = \frac{W\mu}{L}\int_{V_S}^{V_D} Q_i dV = \frac{W\mu}{L}\int_{Q_S}^{Q_D} Q_i \cdot \frac{dV}{dQ_i} \cdot dQ_i. \quad (9)$$

The only information we need to find out the current is $\frac{dQ_i}{dV}$, that is how charge changes with respect to the channel potential. From (8) we have

$$\frac{dQ_i}{dV} = -\frac{dQ_{ieq}}{dV_{CM}}. \quad (10)$$

We see that because of the unique symmetry between the common mode voltage and the channel potential, the current can be calculated from the equilibrium electrostatics relations. Now we have to express $\frac{dQ_{ieq}}{dV_{CM}}$ as a function of charge Q_i. We start by deriving an integral representation of Poisson equation, which will be used later to obtain the expression of $\frac{dQ_{ieq}}{dV_{CM}}$.

3 Integration of Poisson equation

In case of an undoped channel, the electrostatics can be described by the Poisson equation

$$\frac{d^2\Psi}{dx^2} = \frac{qn_i}{\varepsilon_{si}} e^{\frac{\Psi}{U_T}} \quad (11)$$

Defining the normalized quantities:

$$\psi = \frac{\Psi}{U_T}, \quad \xi = \frac{x}{t_{si}}, \quad L_D = \sqrt{\frac{U_T \varepsilon_{si}}{qn_i}} \quad \text{and} \quad U_T = \frac{kT}{q}, \quad (12)$$

relation (11) becomes, in normalized form

$$\frac{d^2\psi}{d\xi^2} = \frac{t_{si}^2}{L_D^2} e^{\psi}. \quad (13)$$

Integrating the equation leads to

$$\frac{1}{2}\left(\frac{d\psi}{d\xi}\right)^2 - \frac{1}{2}\left(\frac{d\psi_r}{d\xi}\right)^2 = \frac{t_{si}^2}{L_D^2}\left(e^{\psi} - e^{\psi_r}\right), \quad (14)$$

where ψ_r is the normalized potential at some reference point. We define

$$C = e^{\psi} - \frac{1}{2}\frac{L_D^2}{t_{si}^2}\left(\frac{d\psi}{d\xi}\right)^2. \quad (15)$$

Note that C is invariant over the vertical position and it is nothing but the constant of the integration. Therefore, (14) now becomes

$$\left(\frac{d\psi}{d\xi}\right)^2 = 2\frac{t_{si}^2}{L_D^2}\left(e^{\psi} - C\right). \quad (16)$$

The important point about C is that it changes sign as the gate voltages are varied. Now let us consider C at the center of the silicon film. When the common mode gate voltage is low, the potential at the middle of the channel is also low and the electric field is high. So C is negative at low gate voltage. As the common mode gate voltage increases the term begin to decrease in magnitude. At high gate voltage, when both channels are inverted, the potential has the U shape. It

implies that the derivative of potential at the middle of the channel is small and C becomes positive.

Now we will use the above equations to obtain a charge based model. At the front(back) interface, the continuity of the displacement vector leads to

$$\frac{\varepsilon_{ox}}{t_{ox}}(V^*_{Gf(b)} - \Psi_{f(b)}) = \varepsilon_{si} \left.\frac{d\Psi}{dx}\right|_{f(b)}. \tag{17}$$

In normalized form it reduces to

$$\frac{\varepsilon_{ox}}{t_{ox}}(v^*_{gf(b)} - \psi_{f(b)}) = \frac{\varepsilon_{si}}{t_{si}} \left.\frac{d\psi}{d\xi}\right|_{f(b)}. \tag{18}$$

For simplicity, we now assume that both gates have the same oxide thicknesses. However, the basic methodology is not limited to this special case and can also be extended to include different gate oxide thicknesses. We now define dimensionless quantities $q_{f(b)} = v^*_{gf(b)} - \psi_{f(b)}$, which represent the charge $Q_{f(b)}$ in the front(back) gate normalized by $C_{ox} \cdot U_T$, where $C_{ox} = C_{oxf} = C_{oxb}$. These two quantities define the total normalized mobile charge q_i as $q_i = q_f + q_b$. When the device operates in WI q_f and q_b have different signs and approximately equal in magnitude (this is because the field inside the silicon film is constant). In SI q_f and q_b have the same sign and revert to the charge sheet representation largely adapted in bulk MOSFET. From (18) we have

$$q^2_{f(b)} = \left(\frac{\varepsilon_{si}}{\varepsilon_{ox}}\right)^2 \left(\frac{t_{ox}}{t_{si}}\right)^2 \left(\left.\frac{d\psi}{d\xi}\right|_{f(b)}\right)^2. \tag{19}$$

Substituting $\frac{d\psi}{d\xi}$ from (16), we can write

$$q^2_{f(b)} = 2\left(\frac{\varepsilon_{si}}{\varepsilon_{ox}}\right)^2 \left(\frac{t_{ox}}{t_{si}}\right)^2 \left(\frac{t_{si}}{L_D}\right)^2 \left(e^{\psi_{f(b)}} - C\right), \tag{20}$$

or

$$\psi_{f(b)} = \ln\left(\frac{q^2_{f(b)}}{2(\frac{\varepsilon_{si}}{\varepsilon_{ox}})^2(\frac{t_{ox}}{L_D})^2} + C\right). \tag{21}$$

Using $v^*_{gf(b)} - \psi_{f(b)} = q_{f(b)}$ we obtain

$$v^*_{gf(b)} = q_{f(b)} + \ln\left(q^2_{f(b)} + 2a^2C\right) - \ln(2a^2). \tag{22}$$

Where $a = \frac{\varepsilon_{si}}{\varepsilon_{ox}}\frac{t_{ox}}{L_D}$.

Note that C is still a function of the gate voltages and hence of the inversion charge.

4 Charge-based expression of $\frac{dQ_{ieq}}{dV_{CM}}$

In this section , we propose to use three asymptotic regions of operation, namely both interfaces in weak inversion, only one interface in strong inversion and both interfaces in strong inversion, to find a charge based approximation of $\frac{dQ_{ieq}}{dV_{CM}}$.

4.1 Both interfaces in weak inversion

In WI we can assume that there is a constant electric field $E = -\frac{d\Psi}{dx}$ in the silicon film. Then the total charge Q_i in WI can be written as

$$Q_i = -\frac{1}{E}\int_{\Psi_f}^{\Psi_b} qn_i e^{\frac{\Psi}{U_T}} d\Psi = \frac{qn_iU_T}{E}\left(e^{\frac{\Psi_f}{U_T}} - e^{\frac{\Psi_b}{U_T}}\right). \tag{23}$$

As inversion charge is very small inside the silicon, we can consider the oxide-silicon-oxide as a capacitive divider and write E as

$$E = \frac{2V_{DM}}{t_{si} + 2(\frac{\varepsilon_{si}}{\varepsilon_{ox}})t_{ox}}. \tag{24}$$

In addition, since E is constant along the film thickness we can notice from (23) that

$$Q_i = \frac{qn_iU_T}{E} e^{\frac{\Psi_f}{U_T}}\left(1 - e^{\frac{-Et_{si}}{U_T}}\right). \tag{25}$$

The main point is that we can write $Q = Ke^{\frac{\Psi_f}{U_T}}$, where K does not depend on the common mode gate voltage. So for the asymmetric case, in WI, we have in normalized form

$$\frac{dq_i}{dv_{cm}} = q_i\frac{d\psi_f}{dv_{cm}}. \tag{26}$$

Since we can approximate our system as a capacitive divider, ψ_f becomes

$$\psi_f = \frac{C_{si} + C_{ox}}{2C_{si} + C_{ox}}v^*_{gf} + \frac{C_{si}}{2C_{si} + C_{ox}}v^*_{gb} = v_{cm} + \frac{C_{ox}}{2C_{si} + C_{ox}}v_{dm}, \tag{27}$$

where C_{si} is the silicon capacitance. This implies $\frac{d\psi_f}{dv_{cm}} = 1$ and for asymmetric DG also, we have $\frac{dq_i}{dv_g} = q_i$ or $\frac{dv_g}{dq_i} = 1/q_i$. The final result then becomes

$$\frac{dq_i}{dv_{cm}} = q_i \quad \text{or} \quad \frac{dv_{cm}}{dq_i} = \frac{1}{q_i}. \tag{28}$$

4.2 Only one interface in strong inversion

Now we will consider the case where only the front gate is inverted. In order to analyze the situation, we will make two assumption. (i) charge sheet approximation at front gate (ii) ignore the volumetric inversion.

If we ignore the volumetric inversion then

$$\frac{d\psi}{d\xi} \simeq \psi_b - \psi_f. \tag{29}$$

Now when only the first gate is inverted the integration constant C can be well approximated by $C \approx -\frac{1}{2}(\frac{L_D}{t_{si}})^2 \cdot (\frac{d\psi}{d\xi})^2$ (C is independent of position and consider the situation at back gate where band bending is so small that it's contribution to C can be neglected). Since the back gate is in weak

inversion, we have (from the continuity of displacement vector in the back interface)

$$C_{ox}(v^*_{gb} - \psi_b) \simeq C_{si}(\psi_b - \psi_f). \tag{30}$$

From the above equation we have

$$\psi_b = \frac{C_{si}}{C_{si} + C_{ox}}\psi_f + \frac{C_{ox}}{C_{si} + C_{ox}}v^*_{gb} \tag{31}$$

(29) now becomes

$$\frac{d\psi}{d\xi} = \frac{C_{ox}}{C_{si} + C_{ox}}(v^*_{gb} - \psi_f) \tag{32}$$

Using the definition $q_f = v^*_{gf} - \psi_f$ we obtain

$$\frac{d\psi}{d\xi} = \frac{C_{ox}}{C_{si} + C_{ox}}(q_f - 2v_{dm}). \tag{33}$$

Using the definition $q_b = v^*_{gb} - \psi_b$ form (31) we have

$$q_b = \frac{C_{si}}{C_{si} + C_{ox}}(q_f - 2v_{dm}). \tag{34}$$

We will now define all quantities in terms of $q_i = q_f + q_b$. For convenience we define $\alpha = \frac{C_{si}}{C_{si}+C_{ox}}$. Using the fact that $q_i = q_f + q_b$, we obtain

$$q_f = \frac{q_i + 2\alpha v_{dm}}{1 + \alpha} \tag{35}$$

$$\frac{d\psi}{d\xi} = \frac{1 - \alpha}{1 + \alpha}(q_i - 2v_{dm}) \tag{36}$$

Using $2a^2C \simeq 2(\frac{\varepsilon_{si}}{\varepsilon_{ox}})^2(\frac{t_{ox}}{L_D})^2\frac{1}{2}(\frac{L_D}{t_{si}})^2(\frac{d\psi}{d\xi})^2$ and $\frac{\varepsilon_{si}}{\varepsilon_{ox}}\frac{t_{ox}}{t_{si}}(1 - \alpha) = \alpha$, we have from (22)

$$v_{cm}+v_{dm} = \frac{q_i + 2\alpha v_{dm}}{1 + \alpha} + \ln\left(q_i^2 + 4\frac{C_{si}}{C_{ox}}v_{dm}q_i\right) + const. \tag{37}$$

From (37), we get

$$\frac{dv_{cm}}{dq_i} = \frac{1}{1 + \alpha} + \frac{2q_i + 4\frac{C_{si}}{C_{ox}}v_{dm}}{q_i^2 + 4\frac{C_{si}}{C_{ox}.}v_{dm}q_i} \tag{38}$$

To find out the charge when the transition between only one inverted surface and two inverted surfaces takes place, we consider that at this point the front surface will be strongly inverted and contribute to most of the charge. These observations allows us to write

$$Q_i \approx C_{ox}(V^*_{Gf} - \Psi_p), \tag{39}$$

where Ψ_p is the pinch-off value of the surface potential. To obtain the value of V_G at this point, we notice that at the back surface (which is now at the edge of inversion), continuity of displacement vector is still applicable and by the definition of inversion $\Psi_b = \Psi_p$. This implies

$$C_{si}(\Psi_p - \Psi_p) = C_{ox}(V^*_{Gb} - \Psi_p) = 0. \tag{40}$$

Eliminating V_G gives the transition charge Q_{tran} as

$$Q_{tran} = C_{ox}(V^*_{Gb} - V^*_{Gf}) = 2C_{ox}V_{DM}. \tag{41}$$

In normalized form q_{tran} is simply twice the difference mode voltage, $q_{tran} = 2v_{dm}$.

4.3 Both interfaces in strong inversion

When both of the surfaces are inverted the potential has a 'U' shape. So the integration constant can be directly associated to the minimum band bending (C is invariant over position and at the point of minimum band bending $\frac{d\psi}{d\xi} = 0$). Then in strong inversion we can ignore the term $2a^2C^2$ compared to q_f^2 and q_b^2. Since the term $q^2_{f(b)} + 2a^2C^2$ appears inside a log term (and C is positive) its impact is anyway small. So in SI from (22) we have

$$v^*_{gf(b)} = q_{f(b)} + 2\ln(q_{f(b)}) + const. \tag{42}$$

Adding these two equations we get

$$2v_{cm} \approx q_f + q_b + 2\ln(q_f q_b) + const. \tag{43}$$

Asymptotically we can assume that $q_f \approx q_b$ inside the log term (RHS of (43) is dominated by the linear term, the impact of the log term is anyway not significant). Therefore in SI, we have

$$2v_{cm} = q_i + 4\ln(q_i) + const. \tag{44}$$

Which directly leads to the simple relation

$$\frac{dv_{cm}}{dq_i} = \frac{1}{2} + \frac{2}{q_i}. \tag{45}$$

4.4 Interpolation of $\frac{dv_{cm}}{dq_i}$

Having calculated $\frac{dv_{cm}}{dq_i}$ in the three regions of operation, we have to combine all the expressions in order to build up a continuous analytical formulation valid in all modes of operation, and that still retains the asymptotic behavior. For the sake of clarity, we will recall the main results hereafter. In WI we have

$$\frac{dv_{cm}}{dq_i} = \frac{1}{q_i}.$$

When only the front surface is inverted ($q_i < 2v_{dm}$) we have

$$\frac{dv_{cm}}{dq_i} = \frac{1}{1 + \alpha} + \frac{2q_i + 4\frac{C_{si}}{C_{ox}}v_{dm}}{q_i^2 + 4\frac{C_{si}}{C_{ox}.}v_{dm}q_i}.$$

And when both the surfaces are strongly inverted we have

$$\frac{dv_{cm}}{dq_i} = \frac{1}{2} + \frac{2}{q_i}.$$

We also have an excellent approximation of $\frac{dv_{cm}}{dq_i}$ for the symmetric case ($v_{dm} = 0$) [3]

$$\frac{dv_{cm}}{dq_i} = \frac{1}{2} + \frac{2q_i + 4\frac{C_{si}}{C_{ox}}}{q_i^2 + 4\frac{C_{si}}{C_{ox}}q_i}. \tag{46}$$

We now propose the following interpolation function between the different asymptotic forms

$$\frac{dv_{cm}}{dq_i} = \frac{1}{1 + \alpha} + \left(\frac{1}{2} - \frac{1}{1 + \alpha}\right)\frac{q_i^n}{q_i^n + \lambda(2v_{dm})^n} + \frac{2q_i + 4\frac{C_{si}}{C_{ox}}(v_{dm} + 1)}{q_i^2 + 4\frac{C_{si}}{C_{ox}}(v_{dm} + 1)q_i}, \tag{47}$$

where n and λ are the interpolation parameters. Note that when $v_{dm} = 0$ the above expression reduces to (46) thus retaining the asymptotic behavior in the symmetrical operation. Now when q_i is very small the RHS of (47) reduces to $1/q_i$. As long q_i remains small compared to $v_{dm} = 0$ the contribution from the 2nd term in the RHS of (47) is very small. In this region we get back the behavior described by (38). As q_i exceeds $2v_{dm}$, the asymptotic of the RHS of (47) becomes $1/2 + 2/q_i$.

4.5 A closed form expression of current

In our implementation we have chosen $n = 4$ and $\lambda = \frac{1}{2}$. This choice provides a reasonably simple expression of the current with acceptable accuracy. The expression of the current becomes $I_D = I_{spec}\left(i_0(q_s) - i_0(q_d)\right)$, where

$$
\begin{aligned}
i_0(q_i) &= \frac{q_i^2}{4} + 2q_i \\
&- \sqrt{2}\cdot\left(\frac{1}{2} - \frac{1}{1+\alpha}\right)\cdot(v_{dm})^2\cdot tan^{-1}\left(\frac{q_i^2}{2\sqrt{2}(v_{dm})^2}\right) - \\
&4\frac{C_{si}}{C_{ox}}(v_{dm}+1)\ln\left(q_i + 4\frac{C_{si}}{C_{ox}}(v_{dm}+1)\right)
\end{aligned}
\tag{48}
$$

and $I_{spec} = \mu C_{ox}\frac{W}{L}U_T^2$.

This analysis provides the current if the charges at the source and drain are known. These charges can be found by solving two coupled nonlinear equations at both ends [1]. However, the equations can be decoupled if one integrates the expression of $\frac{dv_{cm}}{dq_i}$. This requires the evaluation of charge q_i at $v_{cm} = 0$ (the integration constant) in terms of technological parameters and difference mode voltage, which can be easily done by using (25),(27) and the value of $E = \frac{2V_{DM}}{t_{si}+2(\frac{\varepsilon_{si}}{\varepsilon_{ox}})t_{ox}}$ in WI.

5 Results and Discussions

In order to validate the semi-empirical expression given by (48) we compare the analytic expression with exact numerical integration [1], [2]. In our validation we will take a DG MOST with equal and opposite work functions ($\Delta_b = -\Delta_f$) for both gates and tie both gates to a common voltage (this kind of configuration is sufficient because $\Delta_{f(b)}$ actually represents the difference mode of effective gate voltages).

Fig.3 shows the plots of I_D vs V_{GS} (lin and log scales) for different values of the work-function asymmetry ($\Delta_b = -\Delta_f$=0.5, 0.25 and 0 V). The plots show that by increasing the asymmetry, it is possible to have more current in weak and moderate inversion. This is an expected behavior because higher asymmetry implies higher value of charge at low inversion level, hence higher current. But at higher gate voltages the effect of asymmetry vanishes. This can be explained by noticing that at higher gate voltage the device acts as two separate MOST operating in parallel. The inversion charge at each surface has a linear variation with effective gate voltage, so the total charge only depends on the common mode voltage and is independent of difference mode voltage (asymmetry). The plots show very good agreement in both lin and log scale. The excellent match in log scale shows that the transition between strong and weak inversion is very well captured by the single analytical expression. However, a very small (but acceptable) discrepancy is observed around $V_G = \Delta_b - \Delta_f$ in linear scale. This is because of the interpolative nature of the model in this region.

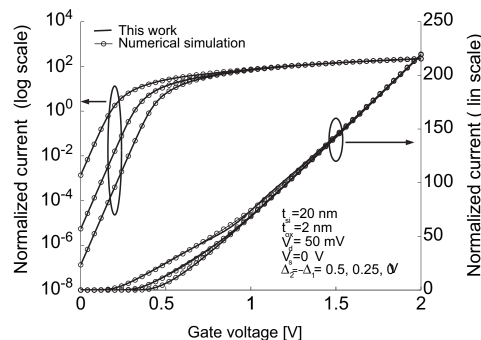

Figure 3: Plot of $I_D$vs V_G in linear region of operation. The current is higher for higher asymmetry ($\Delta_b - \Delta_f$)

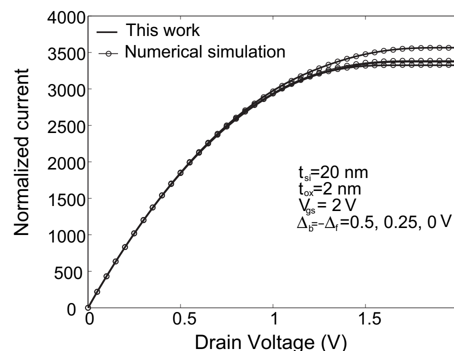

Figure 4: Plot of I_D vs V_G in saturation region of operation. The current is higher for higher asymmetry ($\Delta_b - \Delta_f$)

Next I_D vs V_{DS} is calculated for different values of the effective gate voltage asymmetry ($\Delta_b = -\Delta_f$=0.5, 0.25 and 0 V) and plotted in Fig 4. In saturation, contrary to the linear region behavior in Fig. 3, the current starts to depend on the work-function asymmetry even at high gate voltages. This is because the presence of the channel potential forces some portion of the channel into moderate or weak inversion, where the charge(and the current also, since it is the integral of the charge over the channel potential) depends on the differential mode voltage. These plots also exhibit a very good concordance.

The effect of the silicon film thickness is illustrated for a given value of effective gate voltage asymmetry in Fig.5. The plot shows I_D vs V_{DS} in saturation for different silicon film thickness (t_{si}= 10, 15, 25, 30 nm) for a given value of the work-function asymmetry ($\Delta_b = -\Delta_f$=0.5 V). We observe

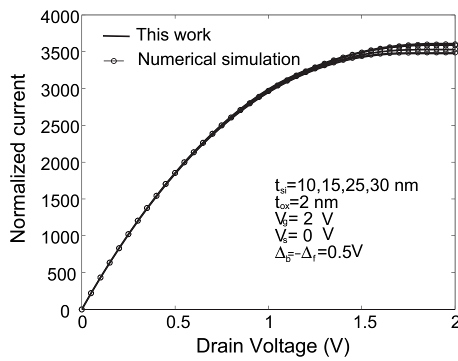

Figure 5: Plot of I_D vs V_G in saturation region of operation. The current is higher for thicker silicon film.

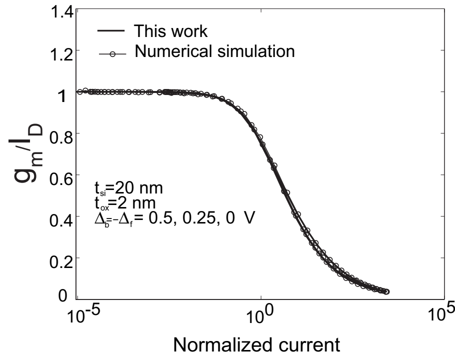

Figure 6: Plot of $\frac{g_m}{I_D}$ vs I_D in saturation region of operation. The ratio is higher for lower asymmetry $(\Delta_b - \Delta_f)$

that the current increases with t_{si}. The reason is mainly that a higher value of t_{si} reduces the 'threshold' of the system by giving a higher value of inversion charge in weak inversion. These plots hence confirm the scalability of our model.

Fig.6 shows the plots of g_m/I_D vs I_D (normalized by I_{spec}) in saturation for different values of the work-function asymmetry ($\Delta_f = -\Delta_b$=0.5,0.25 0 V). As discussed in [4], this special quantity is of great interest for analog IC design. Accuracy between numerical simulations and our analytical approach confirms that the model is also accurate for small-signal analysis. In addition, these results show that although the drain current depends on the work-function difference, the g_m/I_D is almost independent of the asymmetry.

And finally, in order to obtain the terminal charge one needs to solve a coupled nonlinear equation at drain and source ends. Fig. 7 shows the plots for inversion charge vs V_{GS} for both coupled (exact) [1] and de-coupled (approximate, discussed at the end of previous section) solution.

6 Conclusion

In this work we have presented an analytical closed form charge based expression for the drain current of asymmetric DG MOST. Both charge and current are obtained through a

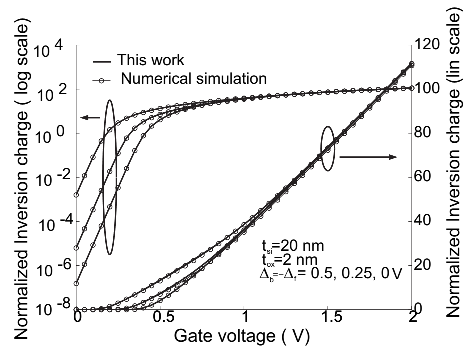

Figure 7: Plot of inversion charge vs V_G in saturation region of operation. The charge is higher for higher asymmetry $(\Delta_b - \Delta_f)$

coherent picture using only the physical parameters of the device and a good matching with exact numerical solution over a wide range of bias and geometry is obtained. In addition, due to its special approach based on a novel interpolation technique in terms of $\frac{dv_g}{dq_i}$, this model can also be extended to small-signal parameter analysis, which is mandatory for an efficient circuit design strategy.

Acknowledgment

The work presented in this paper was supported by the Swiss National Science Foundation under grant number 200021-107971/1.

REFERENCES

[1] Y. Taur, "Analytic solutions of charge and capacitance in symmetric and asymmetric double-gate MOSFET," *IEEE Trans. Electron Devices*, vol. 48, no. 12, pp. 2861 – 2869, Dec. 2001.

[2] Y. Taur, X. Liang, W. Wang, and H. Lu, "A continuous, analytic drain-current model for DG MOSFETs," *IEEE Electron Dev. Let.*, vol. 25, no. 2, pp. 399–401, Feb. 2004.

[3] J. M. Sallese, F. Krummenacher, F. Prgaldiny, C. Lallement, A. Roy, and C. Enz, "A design oriented charge-based current model for symmetric DG MOSFET and its correlation with the EKV formalism," *Solid-State Electronics*, vol. 49, no. 3, pp. 485–489, March 2005.

[4] M. Sylveira, D. Flandre, and P. A. Gespers, " A gm/ID based methodology for the design of CMOS analog circuits and its application to the synthesis of a silicon-on-insulator micropower OTA," *IEEE Journal of Solid-State Circuits*, vol. 31, no. 9, pp. 1314–1319, Sep. 1996.